Adaptive Optics Visual Simulator

Enrique J. Fernández, Msc; Silvestre Manzanera, Msc; Patricia Piers, Msc; Pablo Artal, PhD

ABSTRACT

PURPOSE: To develop a prototype instrument that uses adaptive optics to introduce virtually any desired aberration profile in a subject's eye. At the same time, the instrument could be used to evaluate the subject's spatial vision for each controlled aberration profile. This "aberration testing station" or "visual simulator" allows us to study the relationship between specific aberrations and visual quality.

METHODS: The apparatus uses infrared light to measure the wavefront aberration of the system plus the eye with a Hartmann-Shack wavefront sensor. Defocus is added (or removed) with a computer-controlled, motorized optometer, while higher order aberrations are introduced by a 37-channel membrane deformable mirror. A parallel viewing channel is used for visual testing with the instrument. Visual acuity, contrast sensitivity, and other visual tests are performed under normal viewing for each desired aberration profile.

RESULTS: The range of defocus that can be added is nearly unlimited, while the maximum amount of other aberration modes is restricted to approximately 0.5 µm, depending on mode. Pure modes or any selected combination of modes can be produced with high repeatability and precision (usually better than 0.05 µm), and the system works for pupil diameters up to 6 mm (with a natural pupil).

CONCLUSIONS: The adaptive optics visual simulator is a powerful, non-invasive tool to evaluate how aberrations affect vision. In addition, it can be used for the interactive design and testing of new ophthalmic devices, and for the simulation of visual outcomes in customized refractive surgery. [*J Refract Surg* 2002;18:S634-S638]

From the Laboratorio de Optica, Departamento de Física, Universidad de Murcia, Murcia, Spain (Fernández, Manzanera, Artal) and Pharmacia Groningen, Groningen, The Netherlands (Piers).

Patricia Piers is an employee of Pharmacia; the remaining authors have no proprietary interest in the materials presented herein.

This work was supported by Pharmacia, Groningen, The Netherlands, and MCyT, Spain.

Presented at the 3rd International Congress of Wavefront Sensing and Aberration-free Refractive Correction, February 15-17, 2002, Interlaken, Switzerland.

Correspondence: Pablo Artal, PhD, Laboratorio de Optica, Departamento de Física, Universidad de Murcia, Campus de Espinardo (Edificio C), 30071 Murcia, Spain. Tel: 34.96.8367224; Fax: 34.96.8367667; E-mail: pablo@um.es

Adaptive optics allows real-time correction of the aberrations present in a system. Although initially developed for military and astronomy applications, the use of adaptive optics promises important benefits in visual optics and ophthalmology. The idea of correcting the aberrations of the human eye was first suggested in the early 1960s by Smirnov[1] (most likely independently from the previously proposed application in astronomy). In the late 1980s, the use of a segmented mirror to correct low order aberrations[2] and the application of speckle interferometry in the eye[3] formed the groundwork for present-day research in ophthalmic adaptive optics. More recently, the static correction of ocular aberrations was demonstrated in different laboratories by using deformable mirrors[4] and liquid crystal spatial light modulators.[5] However, due to the dynamic change of ocular aberrations[6], a real-time, closed-loop correction of the aberrations is required if a near-perfect correction is desired. Real-time closed-loop adaptive optics systems for the eye were first reported during the past year.[7,8]

There are a number of areas in ophthalmology in which the use of adaptive optics may have a significant impact. For example, high-resolution ophthalmoscopes allowing resolution of individual retinal cells could be used for early detection of retinal diseases. Another area of interest is related to visual testing—an adaptive optics device can introduce any desired aberration pattern to a subject/patient's eye. We call this concept an adaptive optics visual simulator. By using this type of instrument, it would be possible to test, in advance, the impact on vision of an intended aberration pattern. This will be of specific interest to predict the visual outcomes of wavefront-guided refractive surgery. This approach could also be used in the interactive design of new ophthalmic devices. Finally, from a basic science point of view, it would allow study of the impact of different aberration patterns on spatial vision.

We describe the prototype adaptive optics visual simulator and present examples of wavefront generation in the living eye and the effect on spatial vision.

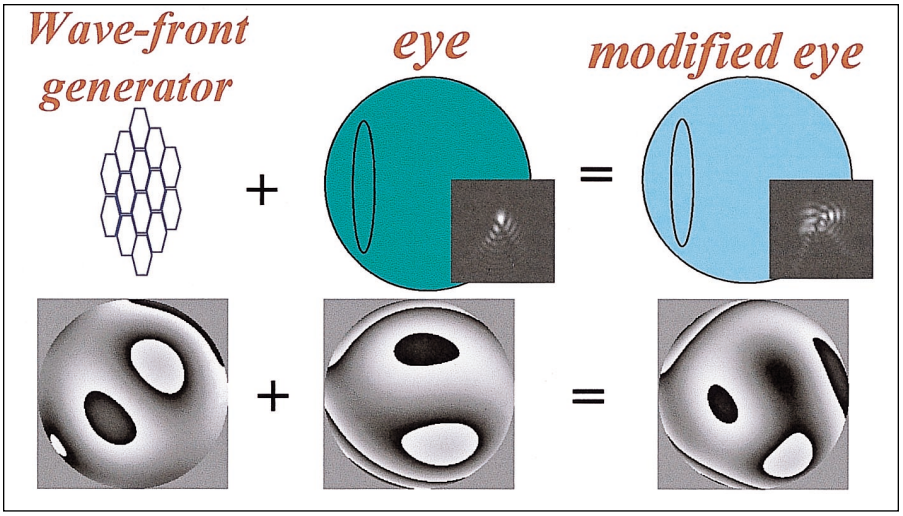

Figure 1. Schematic representation of the principle of the adaptive optics visual simulator (see text for details).

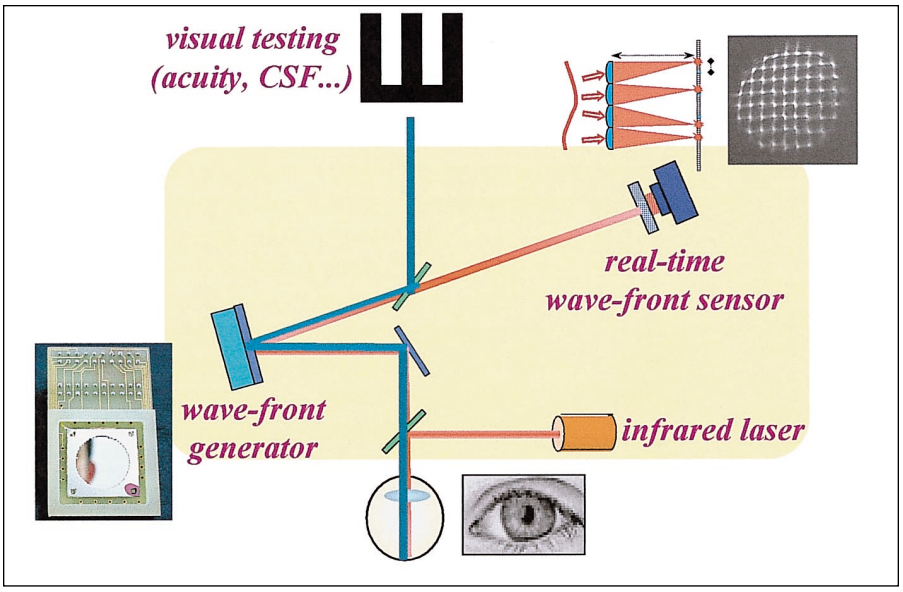

Figure 2. Schematic experimental setup of the adaptive optics visual simulator. A near infrared laser beam illuminates the eye and is focused on the retina. A Hartmann-Shack sensor measures the aberrations in real time and controls the deformable mirror in closed-loop. The deformable mirror compensates or induces aberrations to those present in the subject's eye. By means of an additional beam splitter placed behind the deformable mirror, the subject can see a test with any desired modified aberration pattern.

MATERIALS AND METHODS

Figure 1 presents a schematic description of the operation of the adaptive optics visual simulator. A subject's eye is characterized by an aberration pattern (shown as a gray level wrapped representation) that produces a retinal image (represented as a smaller image in the back of the eye). In this example, the eye has primarily vertical coma. Using a wavefront generator device (in our case, a membrane deformable mirror), a desired aberration pattern is added to the subject's wavefront aberration. The complete system (eye plus generator) has a modified aberration pattern, resulting in a new retinal image. For example, when the wavefront generator produces exactly the same aberration as in the eye, but with opposite sign, the resulting eye will be free of monochromatic aberrations.

Figure 2 shows a schematic of the practical implementation of the adaptive optics simulator. It is based on the real-time, closed-loop adaptive optics device recently developed in our laboratory.[7] A near-infrared (780 nm) diode laser is used for illumination (red line in the diagram). The pupil of the eye is optically conjugated (with lenses not shown for clarity) with both a membrane deformable mirror[9] and with a Hartmann-Shack wavefront sensor[10-12] that is used to measure the ocular aberrations in real time (at 25 Hz). A motorized, computer-controlled optometer (not shown in Fig 2) is used either to correct or to induce defocus. An additional beam splitter, placed after the deformable mirror, allows the subject to see an object (letter chart, grating, etc.) with any desired modified aberration pattern.

The membrane deformable mirror[9] has 37 electrodes under the metallic membrane. It works by electrostatic forces, ie, voltages applied independently to each electrode to induce the required shape of the membrane. To control the deformable

mirror, the membrane's influence functions are first measured. These are the functions that describe the shape of the mirror membrane when a given voltage is applied to each particular electrode. Assuming that the membrane deformation follows a linear superposition of these influence functions, it is straightforward to obtain the required set of voltages to produce a desired mirror shape. This is an iterative process controlled by the continuous measurements of the mirror's shape by the real-time wavefront sensor. The complete process to produce a desired shape in the mirror requires approximately five iterations, corresponding to approximately 0.2 seconds. The use of this type of mirror to generate aberrations presents some advantages: operation in reflection with low-light intensity losses, low power consumption, and especially a relatively low cost, at least in comparison with other deformable mirrors.

However, there are a number of limitations in the use of this mirror for ophthalmic applications of adaptive optics. In particular, due to the number and distribution of the electrodes, not every aberration term can be equally produced, some terms are better replicated than others, and there are important mode-coupling effects. This means that, in general, pure aberration modes are never produced, since low order terms will appear with some amount of the higher order ones that have a similar nature.

Once the aberrations have been modified, a second channel is used for testing the subject's visual quality. Visual acuity, contrast sensitivity, and other visual tests are performed under normal viewing for each desired aberration profile. Patterns were presented in a high resolution monitor using a VSG2/5 visual stimulus generator (Cambridge Research Systems, Kent, England). For visual testing, the presented visual patterns were quasi-monochromatic, centered at 540 nm, by using an interference filter. Since the aberrations were measured in infrared, chromatic longitudinal aberration was compensated by carefully using the motorized optometer, in order to have the eye precisely focused for green light. On the other hand, we assumed that the high order aberrations were relatively stable for different wavelengths. In this way, the aberration pattern (except defocus) we measured in infrared was expected to be relatively similar for green.

Visual acuity was measured by a four-alternate forced-choice illiterate E experiment for high-contrast letters. Subjects press one of four buttons on a keyboard to indicate letter orientation following 250 msec presentations, with one hundred presentations (20 repetitions per five letter sizes) used for each measurement run. The data were then fit to a sigmoid psychometric function, and the 75% probability level was taken as the measure of visual acuity. The visual acuity measurements that we present here were obtained for far vision. The adaptive optics system keeps defocus and aberrations close to the desired levels during the measurements.

Table
Adaptive Optics System Specifications

Hartmann-Shack Wavefront Sensor	
Microlense focal distance	6.3 mm
Microlense size	0.6 mm (square)
Analyzed spots	37
Number of modes measured	21 Zernike terms
Measurements rate	25 Hz
Illumination	Infrared (780 nm)
Pupil size	Up to 5.5 mm
Deformable Mirror (Membrane-type from Okotech)	
Number of electrodes	37
Aperture dimensions	15-mm diameter
Used aperture	9.2-mm diameter
Frequency range	Up to 500 Hz
Maximum deflection	8 μm
Convergence	5 iterations

Pupil size and eye location are monitored by an auxiliary video camera. Because, the current version of the simulator prototype requires precise alignment of the subject's pupil with the deformable mirror, subjects use bite-bars to assure correct and stable centering. However, the system is robust enough for blinking, which ensures the simulator's usefulness for long-duration visual testing. The range of defocus that can be induced is quite large (generated with the motorized optometer). However, the maximum amount of higher order aberration modes that can be produced is approximately 0.5 μm. The actual limit depends on the mode, and is lower for spherical aberrations. Because this can be a significant limitation for some applications, phase plates with different amounts of spherical aberration are placed in the setup in a plane that is conjugated with the eye's pupil, if large values of spherical aberration are required. Pure modes or any combination of modes can be produced with high repeatability and precision (usually better than 0.02 μm), and the system works for pupil diameters up to 6 mm (with a natural pupil). The table summarizes some of the main specifications of the adaptive optics visual simulator.

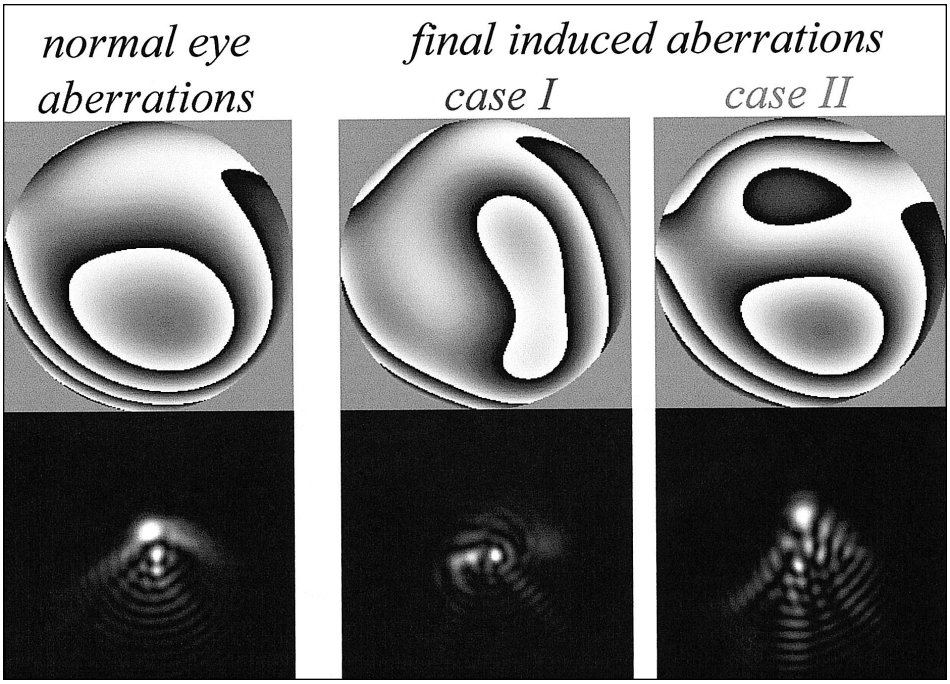

Figure 3. Wave aberration maps and their associated retinal images for the normal eye and the two induced aberrations corresponding to case I and II: different induced aberration pattern with a similar total amount of aberrations and additional coma with the same sign, as present in the eye, respectively.

RESULTS

We used the apparatus to study how different aberration patterns affect spatial vision. In particular, we measured visual acuity, as described, in a normal young subject (SM, one of the authors, 29 years old, with normal vision) for three different aberration patterns. Testing was performed under natural viewing conditions with a pupil diameter of 5.5 mm, and the target placed at infinity. The subject was first asked to find the best subjective refraction by changing the position of the motorized optometer. This was repeated three times prior to initiating the measurements. A precision better than 0.05 diopters (D) was measured for this task. The acuity measurements were then performed for the three following cases: Case N: normal aberrations present in the subject's eye for distant target; Case I: a different induced aberration pattern, with a similar total amount of aberration, but with a significant change in the shape of the retinal image; Case II: additional coma was introduced. This coma had the same sign as the coma that was measured in the subject's eye under normal viewing conditions.

The root mean square (RMS) error for each of the cases were 0.52, 0.42, and 0.48 μm, respectively. For each case, as accommodation was not paralyzed, subjects slightly adjusted (freely) the amount of defocus. Figure 3 shows the wavefront aberration maps and the associated retinal images for the normal eye and the two induced aberration patterns.

From each wavefront aberration, the modulation transfer function (MTF) was estimated. This function can be used to obtain parameters that are indicators of image quality, to be related to visual perception.[13] Figure 4 shows the radially averaged MTFs for the three cases measured. The normal eye and the aberration pattern of Case I are very similar; the aberration pattern of Case II produced a lower MTF. However, what is most interesting is how these three aberration patterns (similar in RMS) affect visual acuity.

Figure 5 presents the visual acuity results (psychometric functions) for the three different aberration patterns. Visual acuity is best (1.3; 20/15) for the subject's normal aberration pattern, but decreases significantly for the aberration pattern of Case I. Additionally, there is a lower reduction in acuity, up to 1.1 (20/18) for the aberration pattern induced in Case II. Thus, despite the fact that the amount of aberration—given by the RMS wavefront errors and the MTFs—was similar in the three cases, the resulting visual acuities were significantly different.

DISCUSSION

We built an adaptive optics visual simulator and demonstrated its potential for use in visual testing for different controlled aberration patterns induced in a subject's eye. The simulator is a powerful and noninvasive tool to evaluate how aberrations affect vision. Important applications are the interactive

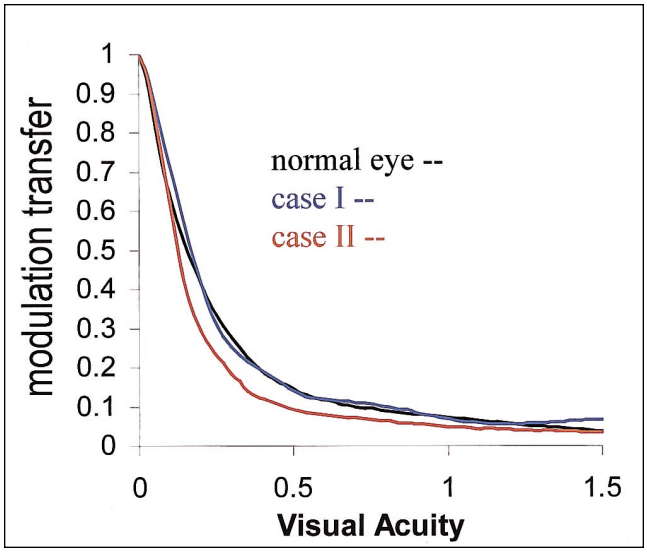

Figure 4. Radial averaged modulation transfer functions (MTFs) for the three cases of induced aberrations. MTFs are plotted as a function of visual acuity in decimal units (1 represents 30 cycles/degree).

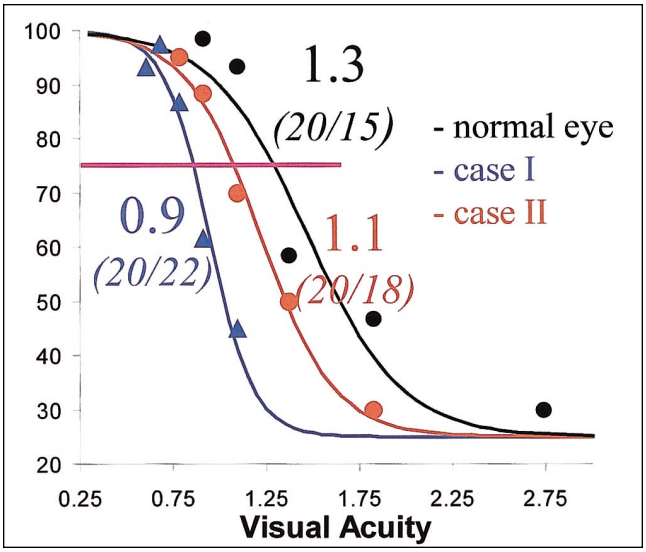

Figure 5. High contrast visual acuity measurements under natural viewing conditions for the three cases of induced aberrations. The percentage of correct responses is plotted as a function of decimal acuity. The visual acuity is set as the value for 75% of the maximum. The case with normal aberrations shows the best visual acuity; visual acuity for cases I and II is lower.

design and testing of new ophthalmic devices, and the simulation of vision previous to customized refractive surgery.

As an example of application of the apparatus, we studied the impact of different aberration patterns on visual acuity. We observed different visual acuity for aberration patterns that were similar in magnitude, but with different orientation. In particular, we measured the best visual performance for the normal aberration pattern in our subject. This may suggest a possible adaptation of the visual system to the normal aberration pattern present in the eye.

REFERENCES

1. Smirnov MS. Measurement of the wave aberration of the human eye. Biofizika 1961;6:776-795.
2. Dreher AW, Bille JF, Weinreb RN. Active optical depth resolution improvement of the laser tomographic scanner. Appl Opt 1989;28:804-808.
3. Artal P, Navarro R. High-resolution imaging of the living human fovea: measurement of the intercenter cone distance by speckle interferometry. Opt Lett 1989;14:1098-1100.
4. Liang J, Williams DR, Miller DT. Supernormal vision and high-resolution retinal imaging through adaptive optics. J Opt Soc Am A 1997;14:2884-2892.
5. Vargas-Martin F, Prieto P, Artal P. Correction of the aberrations in the human eye with liquid crystal spatial light modulators: limits to the performance. J Opt Soc Am A 1998;15:2552-2562.
6. Hofer HJ, Artal P, Singer B, Aragón JL, Williams DR. Dynamics of the eye's wave aberration. J Opt Soc Am A 2001;18:497-506.
7. Fernández EJ, Iglesias I, Artal P. Closed-loop adaptive optics in the human eye. Opt Lett 2001;26:746-748.
8. Hofer H, Chen L, Yoon GY, Singer B, Yamauchi Y, Williams DR. Improvement in retinal image quality with dynamic correction of the eye's aberrations. Optics Express 2001;11:631-643.
9. Vdovin G, Sarro PM. Flexible mirror micromachined in silicon. Appl Opt 1995;34:2968-2972.
10. Liang J, Grimm B, Goelz S, Bille JF. Objective measurement of WA's of the human eye with the use of a Hartmann-Shack wave-front sensor. J Opt Soc Am A 1994;11:1949-1957.
11. Liang J, Williams DR. Aberrations and retinal image quality of the normal human eye. J Opt Soc Am A 1997;14:2873-2883.
12. Prieto PM, Vargas-Martín F, Goelz S, Artal P. Analysis of the performance of the Hartmann-Shack sensor in the human eye. J Opt Soc Am A 2000;17:1388-1398.
13. Villegas EA, González C, Bourdoncle B, Bonnin T, Artal P. Correlation between optical and psychophysical parameters as a function of defocus. Optom Vis Sci 2002;79:60-67.